

DOI: <https://doi.org/10.24425/amm.2024.147777>K. KOŁCZYK-SIEDLECKA^{1*}, D. KUTYŁA¹, K. SKIBIŃSKA¹,
A. JĘDRACZKA¹, P. ŻABIŃSKI¹

CATALYTIC PROPERTIES OF ELECTROLESS NICKEL-BASED COATINGS MODIFIED BY THE MAGNETIC FIELD

In this work the nickel-based coatings were obtained by electroless catalytic deposition on light-hardened resins dedicated for 3D printing by SLA method. The effect of external magnetic field application on the properties of nickel-based coatings was determined. During metallization, the magnetic field was applied to the sample's surface with different orientations. Due to the magnetic properties of metallic ions, the influence of the magnetic field on coatings properties is expected. The coatings were analyzed by Energy-dispersive X-ray spectroscopy (EDS) the X-Ray diffraction (XRD) methods, and surface morphology was observed by scanning electron microscopy (SEM). The catalytic properties in a hydrogen evolution reaction (HER) were measured by electrochemical method in 1 M NaOH solution. The best catalytic activity has been observed in the case of the ternary Ni-Fe-P alloy deposited under a parallel magnetic field. The primary outcome of the presented research is to produce elements based on 3D printing from resins, which can then be metallized and used for highly-active materials deposited on complex 3D models. Furthermore, these elements can be used as low-cost, highly-developed sensors and catalysts for various chemical processes.

Keywords: Electroless deposition; nickel; magnetic field; hydrogen evolution reaction; catalysis

1. Introduction

Additive manufacturing is a technique that is increasingly used in new technologies. For example, the development of the digital revolution and 3D printing methods are changing the way of functional object production [1-4]. The use of 3D printing techniques allows for a quick transition from a digital model to a physical object. This ensures great flexibility in adapting a given geometry, as opposed to classical production methods like machining or casting for metallic parts or injection moulding for plastics. The advantage of this technique is the possibility of producing elements from materials such as plastic, metal or materials based on composites [5-8]. In addition, modification of pieces made by the 3D printing method is used, for example, by modifying the surface by covering it with metallic coatings.

Electroless metallization on non-conductive substrates is a well-known process [9-13]. This technique makes it possible to obtain a combination of metal and plastic properties such as low density or flexibility, conductivity, magnetism or corrosion resistance [14]. One of the state-of-the-art examples of electroless plating is Ni-P deposition. In this process, the

substrate is first cleaned and activated by immersing it in an acidic solution to remove contaminants and promote adhesion. Further, the activated substrate is immersed in a bath containing a solution of nickel ions and a reducing agent, such as sodium hypophosphite [15-17].

The reducing agent reacts with the nickel, which is deposited on the surface of the substrate as a form of the amorphous Ni-P layer according to the multi-stage process. The composition of the Ni-P alloy layer can be controlled by adjusting the concentration of the nickel, phosphorus ions and pH of the electrolyte [18,19] or other process parameters [20,21].

One of the advantages of electroless deposition of Ni-P alloys is that it can deposit a uniform layer on complex geometries, such as internal surfaces of pipes or holes, which is difficult to achieve using traditional electroplating techniques. This method is cheaper than PVD or CVD because no expensive equipment is needed, but well-quality coatings can be obtained. The resulting Ni-P alloy layer also has excellent corrosion resistance, wear resistance, and hardness, making it useful for various industrial applications such as automotive, aerospace, and electronics. Also, electroless metallization processes can easily modify

¹ AGH UNIVERSITY OF KRAKOW, FACULTY OF NON – FERROUS METALS, AL. MICKIEWICZA 30, 30-059 KRAKOW, POLAND

* Corresponding author: kkolczyk@agh.edu.pl



the concentration of elements in coatings by manipulating the composition of electrolytes by adding other elements, such as iron. In the case of Ni-based layers, there is also a possibility to use an external magnetic field due to the ferromagnetic character of ionic species in electrolytes [22].

The magnetic field can be used for electrochemical deposition of thin metallic and alloy coatings based on Ni, Co and Fe [23-27]. An applied magnetic field perpendicular to the surface of the electrode induces the additional Lorentz force, which can modify the transport of ions to the interface [28,29]. This effect was observed in binary and ternary Co-based alloys with molybdenum [30], carbon [31], phosphorous [32]. Orientation of the magnetic field has strongly modified the morphology of deposited layers, which was experimentally proven in the case of Co-Fe layers [33,34]. Moreover, the formation of the localized gradient of the concentration close to the electrode interface has been experimentally and numerically demonstrated [35-37]. Magnetically-induced concentration change has a much more impact on the synthesis of nanostructural materials like Co-Fe nanocones [38,39] or nanowires deposited with the template, where chemical composition can be varied significantly [40]. In this work, we experimentally proved the effect of the magnetic field orientation on the elemental and phase composition of the binary Ni-P and ternary Ni-Fe-P alloys. Differences in the chemical content of elements and morphology of obtained layers significantly affected the catalytic activity of alloys in hydrogen evolution in alkaline solutions. These results show that the magnetic field can be a valuable tool for the design of highly-advanced materials.

2. Experimental

The experimental work used chemicals with analytical purity (ChemLand company). The used substrate was made of FormLabs Form 2 (Clear – GPCL02) resin dedicated to the stereolithography (SLA) method [41].

A liquid resin with a volume of 1 ml was dropped on a glass substrate and then cured using a UV lamp (power 48 W) for 1 minute. The fixed resin samples were washed twice in isopropanol for 20 minutes, according to the manufacturer's instructions. Then, they were washed with demineralized water and dried. The samples were prepared for metallization in a multi-stage process. After each step, the pieces were thoroughly cleaned with demineralized water. First, they were etched in 5% wt. NaOH solution at 70°C for 10 minutes to remove residual resin and other impurities from the surface. Then the samples were placed in a chromic acid solution (30 g/l Cr₂O₃) with the addition of sulfuric acid (80%) for 1 minute at 70°C. Next, the Cr²⁺ ions were removed from the surface in 5% wt. HCl and 5% wt. K₂S₂O₅ solution for 3 minutes at 25°C, then the samples were washed in demineralized water. The surface of resin was activated by Pd²⁺ ions, the samples were placed in 1 g/l PdCl₂ solution for 30 minutes, during this time the ions were adsorbed on resin surface. After this step the sampled were placed in fresh

prepared 20 g/l NaBrH₄ solution to reduce the palladium ions. In this way, the samples were covered with Pd nanoparticles, which is a catalyst in the electroless metallization reactions. The samples prepared in following way were placed in the metallization solutions with the compositions presented in TABLE 1.

TABLE 1

Composition of solution for electroless metallization

| Solution compound | Coating type | |
|--------------------------------------------------------------|---------------------|---------|
| | Ni-P | Ni-Fe-P |
| | concentration [g/l] | |
| NiSO ₄ ·7H ₂ O | 8 | 4 |
| FeSO ₄ ·7H ₂ O | — | 4 |
| NaH ₂ PO ₂ ·H ₂ O | 6 | 6 |
| Na ₃ C ₆ H ₅ O ₇ | 10 | 10 |
| (NH ₄) ₂ SO ₄ | 4 | 4 |
| pH | 9 | 9 |

The pH value was controlled by ammonia solution. The temperature of used solutions was equal to 60°C in every case. The metallization time was equal to 30 minutes.

During the metallization process, the external magnetic field was applied. An electromagnet (LakeShore – Model 642) was used, and a homogeneous magnetic field with an intensity of 0.5 T was generated. The samples surface was oriented perpendicularly or parallelly to the magnetic field lines.

Obtained coatings were analyzed using scanning electron microscopy SEM JEOL – 6000 Plus and XRD Rigaku MiniFlex II. The chemical composition and distribution of elements were determined by EDS analysis.

The catalytic and corrosion properties were analyzed by electrochemical methods. There was used 3-electrode experimental set. The working electrode was coating electroless deposited on resin, the anode was platinum sheet. The reference electrode was the saturated calomel electrode (SCE). Electrochemical measurements were performed in a 1 M NaOH solution at room temperature. The measurements were made as follows: corrosion properties tests by determining Tafel curves, stabilization in open circuit potential (OCP) for 10 minutes, hydrogen evolution curves and determination of galvanostatic curves in the following current densities: –1, –10, –20, –50 mA/cm², every step for 10 minutes. BioLogic SP-200 galvanostat potentiostat was used for electrochemical measurements. To determine the quality of the coatings, SEM pictures of the samples were taken directly as prepared and after the electrochemical tests series.

3. Results and discussion

In the first part of the research work, the time of synthesis of nickel-based alloy coatings was analyzed for elemental composition, corrosion and catalytic properties, and morphology before and after electrochemical tests. First, Ni-P and Ni-Fe-P alloy coatings were deposited on a flat substrate. Then, the composition of the layers was analyzed using the EDS technique.

TABLE 2

Composition of obtained coatings depending on the applied magnetic field

| [% mas.] | 0 T | | \perp 0.5 T | | \parallel 0.5 T | |
|----------|------|------|---------------|------|-------------------|------|
| | P | Fe | P | Fe | P | Fe |
| Ni-P | 4.7 | — | 4.4 | — | 5.2 | — |
| Ni-Fe-P | 5.66 | 7.93 | 5.99 | 7.29 | 6.39 | 7.29 |

The elemental composition of the obtained coatings is shown in TABLE 2. In the case of electroless deposition of the layers, the external magnetic field has no significant effect on the composition of the coatings. In all cases, the phosphorus content ranges from more than 3 to more than 6% by mass.

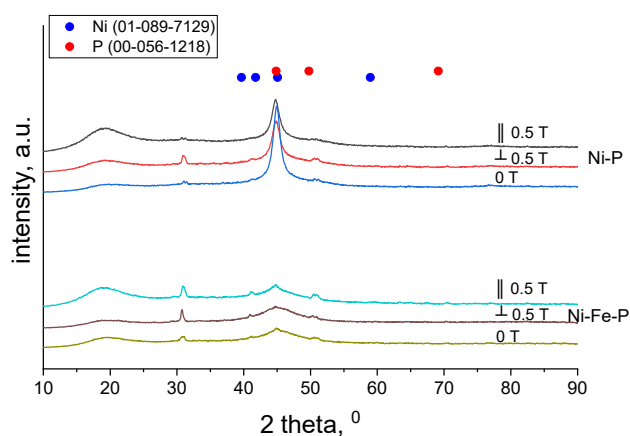
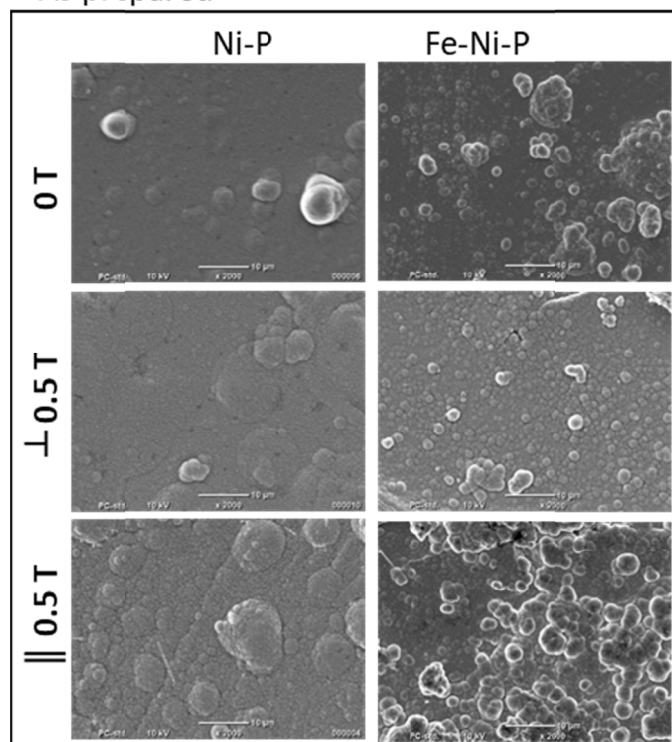


Fig. 1. XRD curves of obtained coatings

Fig. 1 presents the XRD curves of Ni-P and Fe-Ni-P alloy coatings slightly depending on the magnetic field applied during metallization. At the 2θ angle of 45° , peaks from Ni(101) and P(001) were identified. In the case of deposition in a magnetic field, the appearance of a peak at an angle of 50° , assigned to the P(100), was recorded. Based on the many works connected with the Ni-P electroless deposition, obtained XRD diffraction is typical for amorphous-like structure, where the long-distance crystalline structure can be obtained only after proper heat treatment [42,43]. Addition of Iron into ternary Ni-Fe-P coatings are characterized by smaller crystallite sizes, as evidenced by lower and broader peaks. At an angle of 2θ of approx. 31° , a peak was recorded, probably from the holder used for analysis. Obtained layers were also investigated by SEM analysis to detailed study of their morphology and presented in Fig. 2.

In general, the magnetic field greatly influences the diffusion rate of ions during the electroless deposition process and, hence the morphology of the deposit layer. The superimposed magnetic field can strongly increase the movement of the mass transport through the chemical reaction and the deposited layer's properties [28,44,45]. This magnetic field induce the additional Lorentz force which can modify the ion's movement. The acceleration rate is significantly connected with orientation of applied magnetic field. In the case of the applied magnetic field perpendicular to the electrical field lines, the

As prepared

Fig. 2. SEM pictures of alloy coatings before catalytic tests, magnification $\times 2000$

Lorentz force is increasing the diffusion rate, and in the case of the parallel magnetic field their effect in the diffusion rate can be omitted. In term of the ferromagnetic ions like nickel or iron, this effect will be much more intensive, due to the higher magnetic susceptibility. Moreover, after deposition of metals on the electrode, the intensity of formed magnetic gradient will be disrupted, due to the fact that there are a ferromagnetic solid phase in the area of magnetic flux, so the lines of magnetic field will be bended [46]. Presence of highly-graded magnetic field has been experimentally and numerically confirmed, and can be related to different morphological effect on the deposited alloys surface.

When a substrate is placed into the plating solution, palladium clusters present on its surface act as catalysts for reducing nickel ions at specific nucleation sites. Nickel atoms then form and accumulate around these nucleation sites, gradually developing into hemispherical shapes to reduce surface energy. As the deposition process continues, these hemispherical deposits expand until they come into contact with neighboring deposits, ultimately merging to create a continuous film. the nucleation sites are densely and uniformly distributed, they grow to similar small sizes before merging, resulting in a smooth surface coating [47]. The application of a magnetic field with different orientations significantly influences the ion transport to the electrode surface, allowing for customization of the nucleation and growth stage of deposit. In the case of the application of magnetic field, a slightly more developed surface can be seen for parallel magnetic field. Especially, this effect is most visible in the case of the Ni-Fe-P coating, where the formed magnetic

field gradient increase the diffusion rate and allow to form many bigger clusters. This type of structure can exhibit locally higher P concentration, where the overpotential value for hydrogen evolution is the lowest, what was also confirmed in other works [48]. Presence of different morphology with application of the perpendicular and parallel magnetic field can significantly modify the electrochemical performance, like corrosion resistance or electrocatalytic activity [49].

The Tafel curves determined for Ni-P alloys in the potential range from -1.5 V to -0.6 V were presented in Fig. 3. There is no significant magnetic field dependence on the corrosion potential for Ni-P coatings. Coatings are characterized by a similar value of corrosion potential, equal to -0.65 V vs SCE, and similar corrosion current density. Similar investigations were performed for Ni-P, and Ni-Fe-P alloys, presented in Fig. 4.

Comparative analysis for the Ni-P and Ni-Fe-P alloys was performed by measuring the potential onset value and estimating the Tafel slope for the hydrogen evolution reaction. The slope was calculated as the difference between potential values registered for -1 mAcm $^{-2}$ and 10 mAcm $^{-2}$. It can be seen that the lowest value of the onset potential was recorded for ternary Ni-Fe-P alloy deposited under a parallel magnetic field (-1.270 V). The influence of a magnetic field is insignificant in this ternary

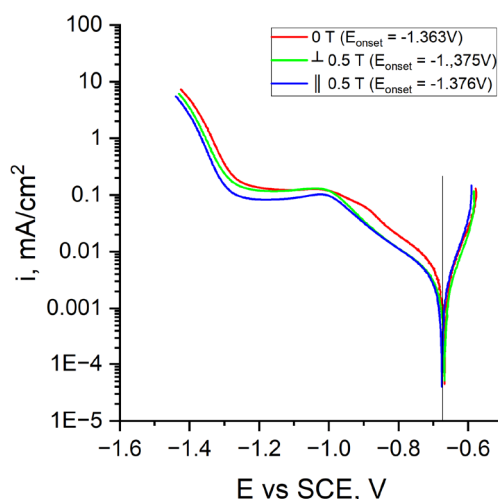


Fig. 3. The Tafel curves determined for Ni-P electroless deposited coatings

alloy because the difference between onset potential for no magnetic field and parallel is only 0.01 V. In the case of Ni-P alloys, the onset potentials were higher (and -1.463 V for Ni-P with no magnetic field). Therefore, applying a magnetic field does not significantly influence the registered potential value. Considering

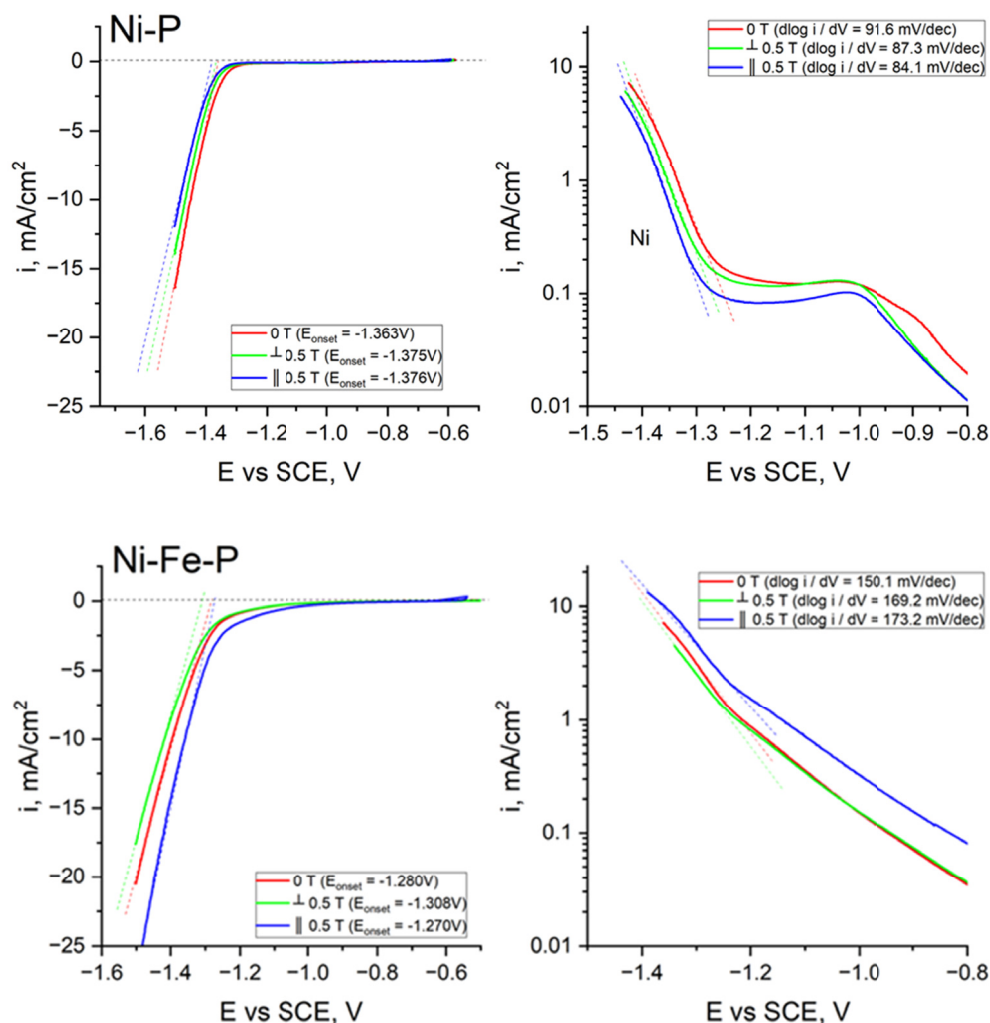


Fig. 4. LSV curves determined for synthesized coatings

the Tafel slope values, the lowest was registered for Ni-P alloys and reached 91 mV dec^{-1} for no magnetic field. It can be seen that the slope value was slightly lower in the case of magnetic field application, 87 and 84 mV dec^{-1} , respectively, for perpendicular and parallel orientation of the magnetic field. Obtained results are in a good correlation with the SEM observations, where any significant changes on the morphology was seen for magnetic field presence. Applying a magnetic field for ternary Ni-Fe-P alloy synthesis increased the tafel slope from 150 mV dec^{-1} to 169 and 173 mV dec^{-1} for perpendicular and parallel magnetic fields, respectively. The Tafel slope increase in ternary alloys can be attributed to the electrode's significantly larger electroactive surface area than in Ni-P deposits. It is clearly confirmed that the catalytic activity of Ni-P and Fe-P alloys is gradually growing with the P concentration [50]. Moreover in case of parallel magnetic field application, there are higher concentration of the phosphorous in alloy, which increase the number of Ni-P nanometrical clusters, which exhibit higher catalytic activity than pure Ni or Fe. Linear voltammetry scans show that the ternary Ni-Fe-P alloys with and without magnetic field are reaching significantly higher cathodic current density for potential -1.5 V than Ni-P deposits. The most significant difference for the parallel magnetic field is -12 mAcm^{-2} and -25 mAcm^{-2} for Ni-Fe-P and Ni-P, respectively. The stability test was performed by applying different cathodic current densities in a range between -1 to -50 mAcm^{-2} , for 600 s and registered the electrode potential variation. The test for Ni-P electrodes deposited without a magnetic field is presented in Fig. 5.

The polarization of the working electrode led to the beginning of the hydrogen evolution reaction. The application of higher current density increased the registered potential value, which reached stable course after 300 s. Similar investigations were also done for Ni-P and Ni-Fe-P alloys obtained without and with a magnetic field with different orientations, listed in TABLE 3.

TABLE 3

Potential values determined in chronoamperometry measurements

| mA/cm ² | Ni-P | | | Ni-Fe-P | | |
|--------------------|-----------|---------|---------|---------|---------|---------|
| | 0 T | ⊥ 0.5 T | ∥ 0.5 T | 0 T | ⊥ 0.5 T | ∥ 0.5 T |
| | E vs. SCE | | | | | |
| -1 | -1.346 | -1.407 | -1.424 | -1.263 | -1.254 | -1.213 |
| -10 | -1.538 | -1.558 | -1.569 | -1.390 | -1.392 | -1.342 |
| -20 | -1.662 | -1.650 | -1.648 | -1.488 | -1.498 | -1.431 |
| -50 | -1.879 | -1.857 | -1.832 | -1.734 | -1.784 | -1.668 |

From the TABLE 3 it can be seen that the presence of magnetic field is profitable for fabrication of materials with increased hydrogen evolution activity. The decrease of registered potentials were observed only in case of application of high current densities (-20 and -50 mAcm^{-2}) for perpendicular and parallel magnetic field. The lowest potential value were registered for Ni-Fe-P alloy, deposited with perpendicular magnetic field. This effect is attributed to highly-developed surface area, where higher number of active sites are present. Similar conclusions

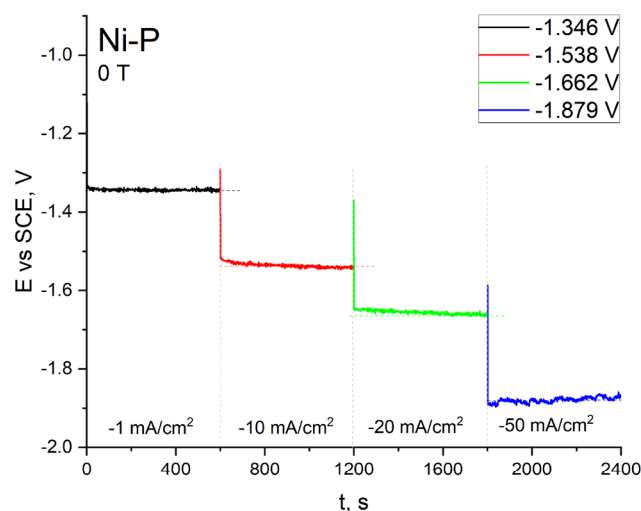
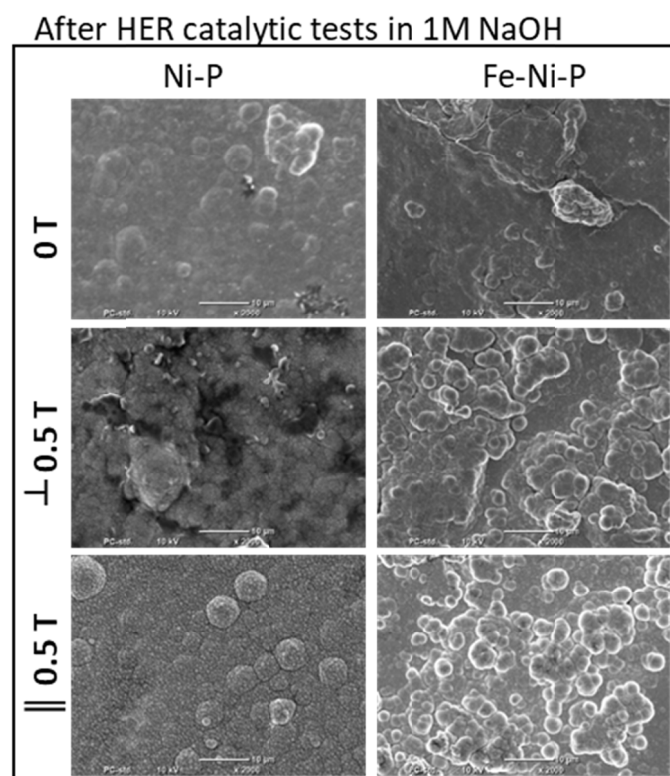


Fig. 5. Chronoamperometry measurements determined for Ni-P coating deposited without external magnetic field

connected with Ni-Fe-P alloys dedicated for water splitting were confirmed for electrochemically-deposited samples in galvanostatic conditions [51]. Moreover it was registered that, the spherical structures are profitable in case of fast formation of small hydrogen bubbles and their detachment from the electrode surface [52,53].

The morphology of alloys after electrocatalytic tests is presented in Fig. 6. Degradation of Ni-P coatings is visible. Ni-Fe-P coatings are characterized by high stability after tests. Their morphology changes not significantly, what makes this

Fig. 6. SEM pictures of alloy coatings after catalytic tests, magnification $\times 2000$

material very promising for application in advanced catalysis based on 3D-printed materials.

4. Conclusions

The aim of this work was the synthesis of nickel-based coatings in electroless metallization processes. The influence of the external magnetic field generated by the electromagnet and applied during the metallization process on the properties of the layers was analyzed. The samples were tested in terms of elemental composition, phase composition, and catalytic properties in the processes of electrochemical hydrogen evolution reaction in 1 M NaOH solution. The morphology was analyzed before and after catalytic tests. During the experimental work, it was found that the external magnetic field has no significant effect on the elemental composition. However, the external magnetic field has a slight impact on the phase composition of the coatings – in the case of using a parallel magnetic field, additional peaks from phosphorus appear in the Ni-Fe-P XRD curves. In addition, slight differences in the electrocatalytic properties of the HER reaction were demonstrated. During chronoamperometric measurements, the coatings were found to be stable during catalytic tests; in the case of using high current densities, a slight change in potential was observed during the measurement. A continuous structure and no cracks on the surface characterized all obtained alloy coatings. After catalytic tests, the Ni-Fe-P coatings surface did not change significantly. It can be concluded that these alloys are characterized by the best properties in terms of application in the HER reaction. This experimental work is the first step in synthesizing composite catalysts based on polymers and metallic alloys. Thanks to 3D printing and metallization, it will be possible to obtain catalysts of any geometry and high catalytic efficiency, with a relatively low density compared to metallic materials.

Acknowledgement

This research was funded by Polish National Science Centre, grant number No UMO- 2017/25/N/ST8/01721. The authors are grateful to Faculty of Non-Ferrous Metals for providing space and materials for research.

REFERENCES

- [1] M. Jiménez, L. Romero, I.A. Dom, M. Dom, Additive Manufacturing Technologies: An Overview about 3D Printing Methods and Future Prospects. *Complexity* **2019**, 9656938 (2019). DOI: <https://doi.org/10.1155/2019/9656938>
- [2] K.V. Wong, A. Hernandez, A Review of Additive Manufacturing. *ISRN Mechanical Engineering* **2012**, 208760 (2012). DOI: <https://doi.org/10.5402/2012/208760>
- [3] M. Attaran, The rise of 3-D printing: The advantages of additive manufacturing over traditional manufacturing. *Bus. Horiz.* **60**, 677-688 (2017). DOI: <https://doi.org/10.1016/j.bushor.2017.05.011>
- [4] T.D. Ngo, A. Kashani, G. Imbalzano, K.T.Q. Nguyen, D. Hui, Additive manufacturing (3D printing): A review of materials, methods, applications and challenges. *Compos. Part B* **143**, 172-196 (2018). DOI: <https://doi.org/10.1016/j.compositesb.2018.02.012>
- [5] B. Derby, Additive Manufacture of Ceramics Components by Inkjet Printing. *Engineering* **1**, 113-123 (2015). DOI: <https://doi.org/10.15302/J-ENG-2015014>
- [6] J.C. Jackson, J.F.C. Windmill, 3D-printing polymer-based permanent magnets, *Mater. Des.* **153**, 120-128 (2018). DOI: <https://doi.org/10.1016/j.matdes.2018.05.005>
- [7] O. Ergeneman, C. Peters, M.R. Gullo, L. Jacot-Descombes, S. Gervasoni, B. Özkale, P. Fatjo, V.J. Cadarso, M. Mastrangeli, S. Pané, et al., Inkjet printed superparamagnetic polymer composite hemispheres with programmed magnetic anisotropy. *Nanoscale* **6**, 10495-10499 (2014). DOI: <https://doi.org/doi:10.1039/c3nr06442e>
- [8] J. Sudagar, J. Lian, W. Sha, Electroless nickel, alloy, composite and nano coatings – A critical review. *J. Alloys Compd.* **571**, 183-204 (2013). DOI: <https://doi.org/10.1016/j.jallcom.2013.03.107>
- [9] J.N. Balaraju, T.S.N. Sankara Narayanan, S.K. Seshadri, Electroless Ni-P composite coatings. *Journal of Applied Electrochemistry* **33**, 807-816 (2003).
- [10] R.A. Shakoar, R. Kahraman, W. Gao, Y. Wang, Synthesis, Characterization and Applications of Electroless Ni-B Coatings-A review. *International Journal of Electrochemical Science* **11**, 2486-2512 (2016).
- [11] M. Żenkiewicz, K. Moraczewski, P. Rytlewski, M. Stepczyńska, B. Jagodziński, Electroless metallization of polymers. *Archives of Materials Science and Engineering* **74**, 67-76 (2015).
- [12] C.A. Loto, Electroless Nickel Plating – A Review, *Silicon* **8**, 177-186 (2016). DOI: <https://doi.org/10.1007/s12633-015-9367-7>
- [13] K. Kolczyk, W. Zborowski, D. Kutyla, A. Kwiecinska, R. Kowalik, P. Zabinski, Investigation of two-step metallization process of plastic 3d prints fabricated by sla method. *Arch. Met. Mater.* **63**, 1031-1036 (2018). DOI: <https://doi.org/10.24425/122438>
- [14] M. Crobu, A. Scorciapino, B. Elsener, A. Rossi, The corrosion resistance of electroless deposited nano-crystalline Ni-P alloys, *Electrochim. Acta* **53**, 3364-3370 (2008). DOI: <https://doi.org/10.1016/j.electacta.2007.11.071>
- [15] S. Bogdach, D. Przybylska, *Poradnik galwanotechnika: Galwaniczne pokrywanie tworzyw sztucznych*, 2002 WNT (Wydawnictwa Naukowo-Techniczne).
- [16] A. Farzaneh, M. Ehteshamzadeh, A.J. Cobley, Modelling of surfactants and chemistry for electroless Ni-P plating. *Surf. Eng.* **34**, 454-461 (2017). DOI: <https://doi.org/10.1080/02670844.2017.1287621>
- [17] J.K. Pancreicious, S.B. Ulaeto, R. Ramya, T.P.D. Rajan, B.C. Pai, Metallic composite coatings by electroless technique – a critical review. *Int. Mater. Rev.* 488-512 (2018). DOI: <https://doi.org/10.1080/09506608.2018.1506692>

- [18] M. Moniruzzaman, S. Roy, Effect of pH on electroless ni-p coating of conductive and non-conductive materials. *Int. J. Automat. Mech. Eng.* **4**, 481-489 (2011).
- [19] X. Wang, W. Cai, W. Wang, H. Liu, Z. Yu, Effects of ligands on electroless Ni-P alloy plating from alkaline citrate – ammonia solution. *Surf. Coatings Technol.* **168**, 300-306 (2003).
- [20] H. Ashassi-Sorkhabi, S.H. Rafizadeh, Effect of coating time and heat treatment on structures and corrosion characteristics of electroless Ni-P alloy deposits. *Surf. Coatings Technol.* **176**, 318-326 (2004). DOI: <https://doi.org/10.1016/S0257-8972>
- [21] A. Chakraborty, N.M. Nair, A. Adekar, P. Swaminathan, Templated electroless nickel deposition for patterning applications. *Surf. Coat. Technol.* **370**, 106-112 (2019). DOI: <https://doi.org/10.1016/j.surfcoat.2019.04.088>
- [22] K. Kołczyk-Siedlecka, K. Skibińska, D. Kutyla, A. Kwiecińska, R. Kowalik, P. Żabiński, Influence of magnetic field on electroless metallization of 3D prints by copper and nickel. *Arch. Metall. Mater.* **64**, 17-22 (2019). DOI: <https://doi.org/10.24425/amm.2019.126212>
- [23] J.A. Koza, M. Uhlemann, C. Mickel, A. Gebert, L. Schultz, The effect of magnetic field on the electrodeposition of CoFe alloys. *J. Magn. Magn. Mater.* **321**, 2265-2268 (2009). DOI: <https://doi.org/10.1016/j.jmmm.2009.01.036>
- [24] A.M. Białostocka, U. Klekotka, B. Kalska-Szostko, Modulation of iron-nickel layers composition by an external magnetic field. *Chem. Eng. Commun.* **206**, 804-814 (2019). DOI: <https://doi.org/10.1080/00986445.2018.1528239>
- [25] A.M. Białostocka, U. Klekotka, B. Kalska-Szostko, Author Correction: The Effect of a Substrate Material on Composition Gradients of Fe-Ni Films obtained by Electrodeposition (*Sci. Rep.* **10**, 1029 (2020)). DOI: <https://doi.org/10.1038/s41598-019-57363-1>; *Sci. Rep.* **10**, 1-8, 7679 (2020). DOI: <https://doi.org/10.1038/s41598-020-64609-w>
- [26] V.C. Long, U. Saraç, M.C. Baykul, L.D. Trong, S. Țălu, D.N. Trong, Electrochemical Deposition of Fe-Co-Ni Samples with Different Co Contents and Characterization of Their Microstructural and Magnetic Properties. *Coatings* **12**, (2022). DOI: <https://doi.org/10.3390/coatings12030346>
- [27] D. Li, Q. Wang, A. Franczak, A. Levesque, J.-P. Chopart, The Coupled Magnetic Field Effects on the Microstructure Evolution and Magnetic Properties of As-Deposited and Post-Annealed Nano-Scaled Co-Based Films – Part I, Electroplating of Nanostructures, 2015 Intech.
- [28] L.M.A. Monzon, J.M.D. Coey, Magnetic fields in electrochemistry: The Lorentz force. A mini-review. *Electrochem. Commun.* **42**, 38-41 (2014). DOI: <https://doi.org/10.1016/j.elecom.2014.02.006>
- [29] S. Luo, K. Elouarzaki, Z.J. Xu, Electrochemistry in Magnetic Fields. *Angew. Chemie – Int. Ed.* **61** (2022). DOI: <https://doi.org/10.1002/anie.202203564>
- [30] P. Żabiński, K. Mech, R. Kowalik, Co-Mo and Co-Mo-C alloys deposited in a magnetic field of high intensity and their electrocatalytic properties. *Arch. Metall. Mater.* **57**, 127-133 (2012). DOI: <https://doi.org/10.2478/v10172-012-0001-z>
- [31] P. Żabiński, K. Mech, R. Kowalik, Electrocatalytically active Co-W and Co-W-C alloys electrodeposited in a magnetic field. *Electrochim. Acta* **104**, 542-548 (2013). DOI: <https://doi.org/10.1016/j.electacta.2012.11.047>
- [32] Y. Yapontseva, V. Kublanovsky, T. Maltseva, O. Gorobets, R. Gerasimenko, Y. Troshchenkov, O. Vyshnevskiy, Effect of Magnetic Field on Electrodeposition and Properties of Cobalt Superalloys. *J. Electrochem. Soc.* **169**, 062507 (2022). DOI: <https://doi.org/10.1149/1945-7111/ac7898>
- [33] J.A. Koza, M. Uhlemann, A. Gebert, L. Schultz, The effect of magnetic fields on the electrodeposition of CoFe alloys. *Electrochim. Acta* **53**, 5344-5353 (2008). DOI: <https://doi.org/10.1016/j.electacta.2008.02.082>
- [34] J.A. Koza, M. Uhlemann, A. Gebert, L. Schultz, The effect of a magnetic field on the pH value in front of the electrode surface during the electrodeposition of Co, Fe and CoFe alloys. *J. Electroanal. Chem.* **617**, 194-202 (2008). DOI: <https://doi.org/10.1016/j.jelechem.2008.02.009>
- [35] K. Kołczyk, M. Wojnicki, D. Kutyla, R. Kowalik, P. Żabiński, A. Cristofolini, Separation of Ho³⁺ in Static Magnetic Field. *Arch. Metall. Mater.* **61**, 1919-1924 (2016). DOI: <https://doi.org/10.1515/amm-2016-0308>
- [36] K. Kołczyk-Siedlecka, M. Wojnicki, X. Yang, G. Mutschke, P. Zabinski, Experiments on the magnetic enrichment of rare-earth metal ions in aqueous solutions in a microflow device. *J. Flow Chem.* **9**, (2019). DOI: <https://doi.org/10.1007/s41981-019-00039-8>
- [37] K. Kołczyk, D. Kutyla, M. Wojnicki, A. Cristofolini, R. Kowalik, P. Zabinski, Separation of rare earth metals ions in a static magnetic field. *Magnetohydrodynamics* **52**, 541-547 (2016).
- [38] K. Skibińska, D. Kutyla, K. Kołczyk-Siedlecka, M.M. Marzec, P. Żabiński, R. Kowalik, Synthesis of conical Co-Fe alloys structures obtained with crystal modifier in superimposed magnetic field. *Arch. Civ. Mech. Eng.* **21**, 1-11 (2021). DOI: <https://doi.org/10.1007/s43452-021-00315-2>
- [39] M. Huang, K. Skibinska, P. Zabinski, M. Wojnicki, G. Włoch, K. Eckert, G. Mutschke, On the prospects of magnetic-field-assisted electrodeposition of nano-structured ferromagnetic layers. *Electrochim. Acta* **420**, (2022). DOI: <https://doi.org/10.1016/j.electacta.2022.140422>
- [40] S. Mottaghian, M. Najafi, A. Abbas Rafati, S. Ali Asghar Terohid, Structural, morphological, angular dependent of magnetic properties and FORC analysis of CoFeIn novel nanowire alloys. *Mater. Sci. Eng. B Solid-State Mater. Adv. Technol.* **290**, 116334 (2023). DOI: <https://doi.org/10.1016/j.mseb.2023.116334>
- [41] KMK Regulatory Services Inc Clear Photoreactive Resin for Formlabs 3D printers Karta charakterystyki Available online: https://sklep.3dl.tech/wp-content/uploads/2017/12/Clear_Formlabs-SDS-EU-Polish.pdf (accessed on Jun 15, 2019).
- [42] A. Lelevic, F.C. Walsh, Electrodeposition of Ni-P alloy coatings: A review. *Surf. Coatings Technol.* **369**, 198-220 (2019). DOI: <https://doi.org/10.1016/j.surfcoat.2019.03.055>
- [43] D.H. Jeong, U. Erb, K.T. Aust, G. Palumbo, The relationship between hardness and abrasive wear resistance of electrodeposited nanocrystalline Ni-P coatings. *Scr. Mater.* **48**, 1067-1072 (2003). DOI: [https://doi.org/10.1016/S1359-6462\(02\)00633-4](https://doi.org/10.1016/S1359-6462(02)00633-4)

- [44] O'Reilly, G. Hinds, J.M.D. Coey, Effect of a Magnetic Field on Electrodeposition: Chronoamperometry of Ag, Cu, Zn, and Bi. *J. Electrochem. Soc.* **148**, C674 (2001).
DOI: <https://doi.org/10.1149/1.1402121>
- [45] Y. Yang, K.M. Grant, H.S. White, S. Chen, Magneto-electrochemistry of Nitrothiophenolate-Functionalized Gold Nanoparticles. *Langmuir* **19**, 9446-9449 (2003).
DOI: <https://doi.org/10.1021/la0345688>
- [46] Y. Zhang, B. Yuan, L. Li, C. Wang, Edge electrodeposition effect of cobalt under an external magnetic field. *J. Electroanal. Chem.* **865**, 114143 (2020).
DOI: <https://doi.org/10.1016/j.jelechem.2020.114143>
- [47] J.P. Marton, M. Schlesinger, The Nucleation, Growth, and Structure of Thin Ni-P Films. *J. Electrochem. Soc.* **115**, (1968).
DOI: <https://doi.org/10.1149/1.2410991>
- [48] A.P. Gaikwad, A.M. Banerjee, M.R. Pai, R. Dheeman, S. Kumar, A.K. Tripathi, Synthesis, microstructure and electrochemical properties of Ni-P-based alloy coatings for hydrogen evolution reaction in alkaline media. *Mater. Res. Express* **10**, (2023).
DOI: <https://doi.org/10.1088/2053-1591/acf278>
- [49] S. Chouchane, A. Levesque, P. Zabinski, R. Rehamnia, J.-P. Chopart, Electrochemical corrosion behavior in NaCl medium of zinc-nickel alloys electrodeposited under applied magnetic field. *J. Alloys Compd.* **506**, 575-580 (2010).
DOI: <https://doi.org/10.1016/j.jallcom.2010.07.099>
- [50] O.V. Dolgikh, Y.G. Kravtsova, N.V. Sotskaya, The effect of composition of electrodeposited Ni-P alloys on the hydrogen evolution rate. *Russ. J. Electrochem.* **46**, 918-924 (2010).
DOI: <https://doi.org/10.1134/S1023193510080094>
- [51] J. Lian, Y. Wu, H. Zhang, S. Gu, Z. Zeng, X. Ye, One-step synthesis of amorphous Ni-Fe-P alloy as bifunctional electrocatalyst for overall water splitting in alkaline medium. *Int. J. Hydrogen Energy* **43**, 12929-12938 (2018).
DOI: <https://doi.org/10.1016/j.ijhydene.2018.05.107>
- [52] L. Krause, K. Skibińska, H. Rox, R. Baumann, M.M. Marzec, X. Yang, G. Mutschke, P. Żabiński, A.F. Lasagni, K. Eckert, Hydrogen Bubble Size Distribution on Nanostructured Ni Surfaces: Electrochemically Active Surface Area Versus Wettability. *ACS Appl. Mater. Interfaces* (2022).
DOI: <https://doi.org/10.1021/acsami.2c22231>
- [53] R. Hannes, A. Bashkatov, X. Yang, S. Loos, G. Mutschke, G. Gerbeth, K. Eckert, Bubble size distribution and electrode coverage at porous nickel electrodes in a novel 3-electrode flow-through cell. *Int. J. Hydrogen Energy* **48**, 2892-2905 (2023).